DISPERSION ENGINEERED MID-IR SUPERCONTINUUM GENERATION USING DUAL-CORE SILICON-RICH NITRIDE PHOTONIC INTEGRATED WAVEGUIDE

وَمَن يُؤْتَ الحِكْمَةَ
فَقَدْ اُوتِيَ خَيْرًا كَثِيرًا

QUAID-I-AZAM UNIVERSITY

ISLAMABAD

By

Kiran Ilyas

SUBMITTED IN PARTIAL FULFILLMENT OF THE
REQUIREMENTS FOR THE DEGREE OF
MASTER OF PHILOSOPHY
AT
QUAID-I-AZAM UNIVERSITY
ISLAMABAD, PAKISTAN
APRIL 2021

QUAID-I-AZAM UNIVERSITY
DEPARTMENT OF ELECTRONICS

The undersigned hereby certify that they have read and recommend to the Faculty of Graduate Studies for acceptance a thesis entitled "**Dispersion Engineered Mid-IR Supercontinuum Generation Using Dual-core Silicon-Rich Nitride Photonic Integrated Waveguide**" by **Kiran Ilyas** in partial fulfillment of the requirements for the degree of **Master of Philosophy**

Dated: <u>April 2021</u>

Research Supervisor: _____

Chaiman: _____

QUAID-I-AZAM UNIVERSITY

Date: **April 2021**

Author: **Kiran Ilyas**

Degree: **M. Phil.**

Title: **Dispersion Engineered Mid-IR Supercontinuum Generation Using Dual-core Silicon-Rich Nitride Photonic Integrated Waveguide**

Department: **Electronics**

Year: **2021**

Permission is herewith granted to Quaid-I-Azam University to circulate and to have copied for non-commercial purposes, at its discretion, the above title upon the request of individuals or institutions.

_____
Signature of Author

"O my Lord!

Bestow wisdom upon me and join me with the

righteous."

(Qur'an: Surah26, Verse 83.)

Table of Contents

List of Figures

Acknowledgments

I would like to first express my gratitude to my supervisor, Dr. Qaisar Abbas Naqvi, for a valuable experience. The insights and expertise I have gained from him will help me steer through my future career as well. I would like to extend my thanks to all the Professors of my department including: Dr. Azhar Abbas Rizvi, Dr. Muhammad Aqeel Ashraf, Dr. Muhammad Arshad Fiaz, Dr. Muhammad Zia, Dr. Musarat Abbas, and Dr. Arshad Hussain for their immense support and advice during my candidature. Special thanks to Dr. Azhar Abbas Rizvi whose interaction has always been a rewarding experience for me. I would also like to thank the head of the Electronics department, Prof. Dr. Aqeel Abbas, who is very supportive and wants every student to succeed in their academic endeavors.

I would like to express my sincere gratitude to my lab members: Maria Iqbal, Nimra Ali, Fatima Bibi, Kishwar Ali, and Junaid Hassan for their comradeship and joyful lab environment. Special thanks to Maria Iqbal for her support and assistance in time of need. I would also like to thank my friends outside my lab: Usman Hashmi, Sajid Hanif, Ayesha Jabeen, Muqaddas Parvaiz, Mehwish Malik, Iqra Fareed, Qurat-ul-Ain and all the fellows from the department who have been a great support during my research. Special thanks to Sundas Baig and Kiran Amjad who have been very compassionate in listening to my concerns and always motivating me towards positivity. Talking to them was such a stress relief.

I would like to acknowledge the Electronics department of Quaid-i-Azam University for providing me with a fellowship and the opportunity to work in the cutting-edge research environment.

Abstract

The dual-core silicon-rich nitride photonic integrated waveguide is presented here to numerically model the spanning of supercontinuum generation in the mid-IR region up to $4.7\mu m$ wavelength range by engineering the dispersion profile such that maximum phase-matching can be achieved. Tunable dispersive wave generation is observed by the variation of gap spacing between two cores. The flat dispersion profile is also achieved in near-IR region by coupling the fundamental mode in first waveguide core to the higher-order mode in second waveguide core that gives rise to anomalous GVD which plays an essential role in compensating chromatic dispersion in the mid-IR region.

Chapter 1

Introduction

Supercontinuum generation (SCG) is a nonlinear process that has been used for spectral broadening and soliton generation[1]. When a high-intensity light source travels in a nonlinear medium, due to the strong nonlinear interactions it undergoes an intensity-dependent phase shift and it gets modulated by its own phase known as self-phase modulation (SPM) which gives rise to the addition of new frequency components [2][3]. The desired spectral components can then be extracted from the broadband output, for example, using a tunable band-pass filter. That is why it also refers to as a broadband source generation.

Spanning of the SCG in mid-IR region of the electromagnetic spectrum with the main focus on 3 to 5 μm wavelength region is getting more attention of the researchers these days. This particular region is extremely important for many spectroscopy and sensing applications because of the presence of vibrational transitions in molecules under this range of wavelength[4]. There are many mid-IR sources such as integrated cascaded laser (ICL) [5], quantum cascaded laser (QCL)[6][7][8], parametric down-conversion, frequency difference generation[9][10], and diode laser that can be used to perform several applications in this regime. Optical clocks[11], bio-sensing[12], imaging[13], optical coherence tomography[14], frequency metrology[15], and free-space communications[16] are a few applications of supercontinuum sources.

Supercontinuum sources are also used to generate broadband frequency combs which

are important for high-resolution spectroscopy applications. It has also been used on a variety of mid-IR comb sources recently[17][18], such as micro-resonator, Kerr frequency combs[19][20][21], and phase-locked mid-IR frequency combs with high brightness and large bandwidth. Such frequency combs are created from a femto-second (fs) pumped laser source [22] which represent the high peak power of the pulse that leads to the enhancement of nonlinear effects.

Recently, the photonic integrated platform has received a lot of attention such as silicon nanowires[23][24], silica ridge waveguides [25][26], lithium niobate [27][28], aluminum gallium arsenide [29][30], aluminum nitride [31][32], and silicon nitride waveguides[33][34][35] which give access to tighter confinement, strong nonlinearity, dispersion engineering, power-efficient and compact devices at wafer scale.

As mentioned above, the IR region is highly important for spectroscopy. One of the key challenge with chip-based supercontinuum sources is that spectral components generated in this specific band have low power due to relatively high phase mismatch with respect to the pump. The phase-matching process is important because it defines the conservation of energy and momentum of the system. Traditional mid-IR comb sources are based on a single waveguide but these particular structures have issues in achieving high phase matching. In order to resolve this issue, recently, a method has been demonstrated in[36], in which instead of using a single waveguide, two waveguides are placed in close proximity allowing the mode coupling for further dispersion engineering. Hence, by introducing mode coupling especially at the mid-IR range, the phase mismatch can be altered to get enhanced effects of super-continuum in the mid-IR region. However, the supercontinuum spanning was limited up to $4\mu m$ wavelength [35][36]. Other platforms like lithium niobate ($LiNbO_3$) [27][28], aluminum nitride (AlN) [31][32], and aluminum gallium arsenide (AlGaAs) [30][30] also could not extend supercontinuum spanning beyond $4\mu m$. In this thesis, we will consider a photonic integrated dual-core waveguide with silicon-rich nitride (Si_2N) core and lithium niobate ($LiNbO_3$) as cladding of the waveguide to observe the supercontinuum spanning in mid-IR region beyond $4\mu m$ particularly up to $4.7\mu m$ wavelength.

The silicon nitride (Si_3N_4) has been extensively studied in photonic integrated platform because it is compatible with complementary metal-oxide semiconductor (CMOS) technology and has a low propagation loss. On the other hand, it is constrained by its low optical Kerr nonlinearity of about $2.40 \times 10^{-15} cm^2/W$ [37]. In contrast to that, silicon-rich nitride core in our proposed geometry possesses a high refractive index of about 3.16 and strong Kerr nonlinearity of $1.60 \times 10^{-13} cm^2/W$ which is four times larger than that of silicon, and two orders of magnitude greater than that of silicon nitride[37][38]. The high index of refraction allows the optical mode to be more tightly confined in the waveguide, and the stronger Kerr nonlinearity is responsible for achieving broadband supercontinuum generation and enables us to operate with the incident pulse having peak power of around 10W which is very low as compared to the most widely used silicon nitride (Si_3N_4) material which operates at around 4.5kW peak power [36].

Supercontinuum generation critically depends on the dispersion properties which can be engineered by making some significant changes in the geometry of the waveguide such that the maximum phase matching can be achieved for the dual-core waveguide in mid-IR region, leading to the generation of dispersive wave up to $4.7\mu m$ wavelength when the pump field is in the near-IR region particularly at 1550nm wavelength with very low pulse peak power of about 10 W, keeping the pulse time width of 0.95 pico second. The flat dispersion profile is also achieved for some extent in near-IR region using silicon rich nitride (Si_2N) dual-core waveguide structure which is usually tough to achieve in a single-core waveguide structure[38].

The main focus of this thesis is to examine the supercontinuum spanning upto mid-IR region by engineering the dispersion profile of the dual-core waveguide structure. To give a clear idea of the present work, the discussion is divided into two parts. Firstly, the dispersion engineering is discussed in which the waveguide dimensions are tuned to get phase matching up to the desired wavelength in mid-IR region. Secondly, the supercontinuum generation is observed for the dispersion engineered structure. For this intent, simulations are performed on COMSOL Multi-physics software and the

information of the effective refractive indices (n_{eff}) has been collected. The results for both waveguide dispersion (D_{wg}) and integrated dispersion ($\Delta\beta$) has been calculated and at the same time influence of variation of gap spacing between two cores has been discussed. It is highlighted that supercontinuum spanning is extended beyond $4\mu m$ with the closer proximity of the two cores.

Chapter 2

Dispersion Engineering

Silicon rich nitride (Si$_2$N) dual-core waveguide is presented in this thesis which consists of narrow core width of $w_1 = 1.3\mu$m and wide core width of $w_2 = 3\mu$m, with $0.5\mu m$ identical core height and $0.6\mu m$ gap distance between the two cores, embedded in lithium niobate (LiNbO$_3$) cladding. The schematics are shown in figure (2.1). The refractive indices of Silicon rich nitride (Si$_2$N) core and lithium niobate (LiNbO$_3$) cladding are modeled by sellmier equation given by equation (2.0.1) and equation (2.0.2), that are taken from [39] and [40] respectively.

$$n_{\text{core}} = 1 + \sqrt{1 + \sum_{k=1}^{N} \frac{\alpha_k \lambda^2}{\lambda^2 - \beta_k^2}} \tag{2.0.1}$$

$$n_{\text{cladding}} = \sqrt{1 + \sum_{k=1}^{N} \frac{\alpha_k \lambda^2}{\lambda^2 - \beta_k^2}} \tag{2.0.2}$$

where α_k and β_k represent the sellmier coefficients and their values are provided in table (2.1) whereas λ is considered in μm.

The high coupling efficiency from optical fiber to the waveguide can be achieved with lower losses by using inverse taper structure[41] at the input section of the waveguide which is represented in the proposed waveguide structure in figure (2.1). The waveguide mode is not entirely confined to the core of the structure but it also have evanescent tail that extends to the cladding, resulting in an intriguing phenomenon

5
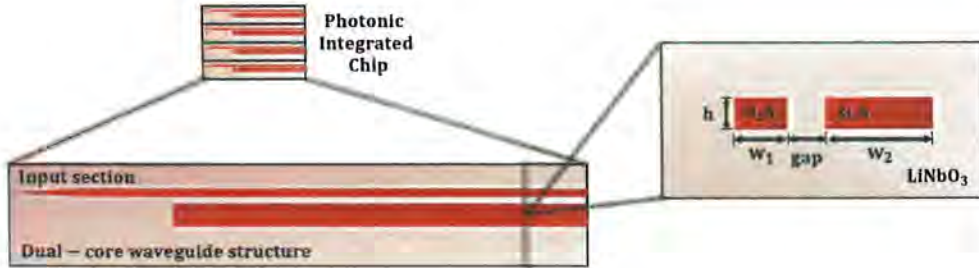
Figure 2.1: Schematic for Si$_2$N dual-core waveguide where input section represents the inverse taper structure and the output section contains dual-core waveguide structure. The cross-section of the waveguide structure is also shown on the left.

Table 2.1: **Sellmeier coefficients for core and cladding materials.**

Materials	Si$_2$N		LiNbO$_3$	
N	α_k	β_k	α_k	β_k
$k = 1$	2.21715	0.0632602	2.67334	0.01764
$k = 2$	1.12108	0.249134	1.2290	0.054914
$k = 3$	24.8224	250.091	12.614	474.600
$k = 4$	17.6617	251.079	-	-

called "evanescent wave coupling". The lowest order mode known as the fundamental mode has the highest field strength in the middle and travels straight through the waveguide core and the propagating evanescent wave travels along the boundary of the core into the cladding. Whereas the higher-order modes experience multiple reflections during the propagation along the waveguide leading to the penetration of mode into the cladding. As the waveguide width increases multiple higher-order modes start to appear, which is why we try to avoid pumping into the wide core. The figure (2.1) explains the fact that the light signal is pumped into the waveguide from the narrow core (top waveguide) and it gets coupled to the wide core placed at the closer proximity to the narrow core. The gap spacing between the two cores can be tuned in order to engineer the integrated dispersion of the waveguide.

As the two waveguide cores are separated by a smaller gap distance of $0.6\mu m$, the mode propagating in one core is most likely to be coupled to the mode of the other core

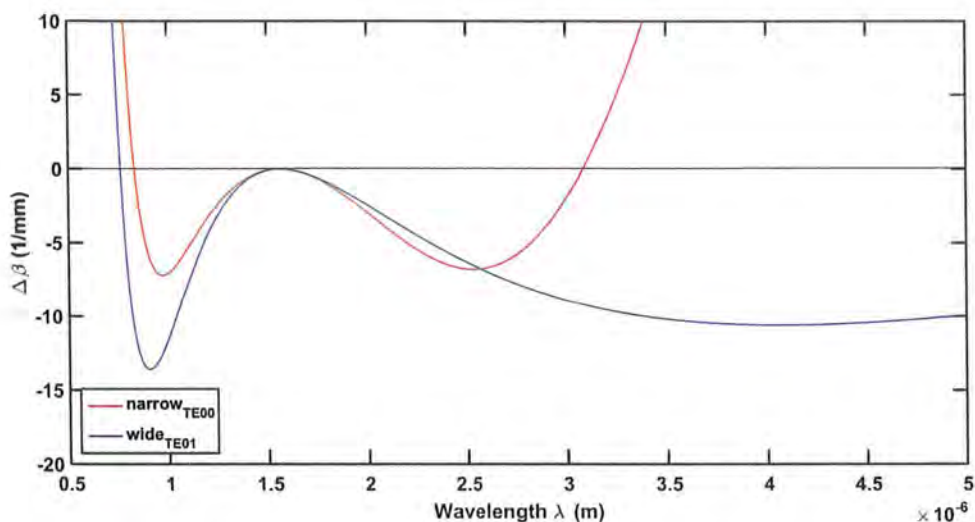Figure 2.5: The integrated dispersion phase profile of fundamental TE00 mode in narrow core and second-order TE01 mode of the wide core are compared for the waveguide with a core height of $0.5\mu m$.
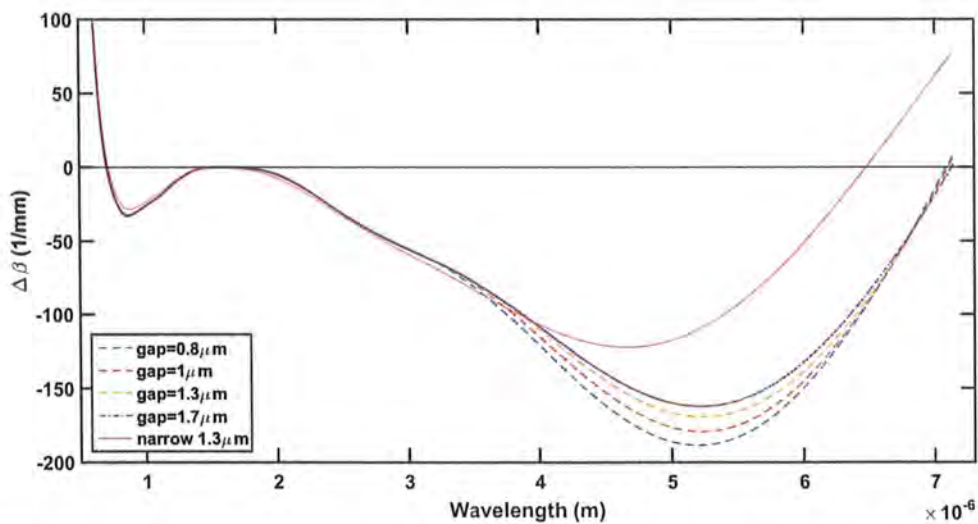
Figure 2.6: The integrated dispersion phase profile for the anti-symmetric mode of dual-core waveguide with core height of $0.8\mu m$ for gap distance changing from $0.8\mu m$ to $1.7\mu m$.

Chapter 3

Spanning of Supercontinuum Generation

Here we are trying to see the combined effect of dispersion (GVD) and nonlinear effects (SPM) on the pulse propagation through a nonlinear medium via nonlinear schrödinger equation (NLSE)[1] which can be solved by symmetrized split-step fourier method (SSSFM)[42][43]. By tuning the waveguide dimensions, the dispersion phase profile can be engineered which facilitates in spanning the broad-band supercontinuum generation in the mid-IR region. The phase propagation constants for supported modes are calculated by performing the FEM simulations using COMSOL Multiphysics software. As the dispersion phase profiles for the anti-symmetric mode of dual-core waveguide with core height of $0.5\mu m$ for gap distance of $0.6\mu m$ have been discussed earlier in section 2.2. The dispersive wave generation was observed up to $4.7\mu m$ wavelength range.

In the simulations performed for supercontinuum generation, the nonlinear Kerr index $n_2 = 1.60e^{-17}m^2/W$ and the value of non-linear factor $\gamma = 206W^{-1}/m$ [37], the peak power of the pump pulse is kept at 10W and the pulse time width as 0.9 picoseconds. The pump pulse is launched into the 15mm long waveguide with 1550nm wavelength. The spectral broadening is initiated at around 5mm length of the waveguide. The spectral evolution can be seen in figure (3.1 a) which illustrates that the supercontinuum is achieved from visible to the mid-IR region particularly from $0.7\mu m$

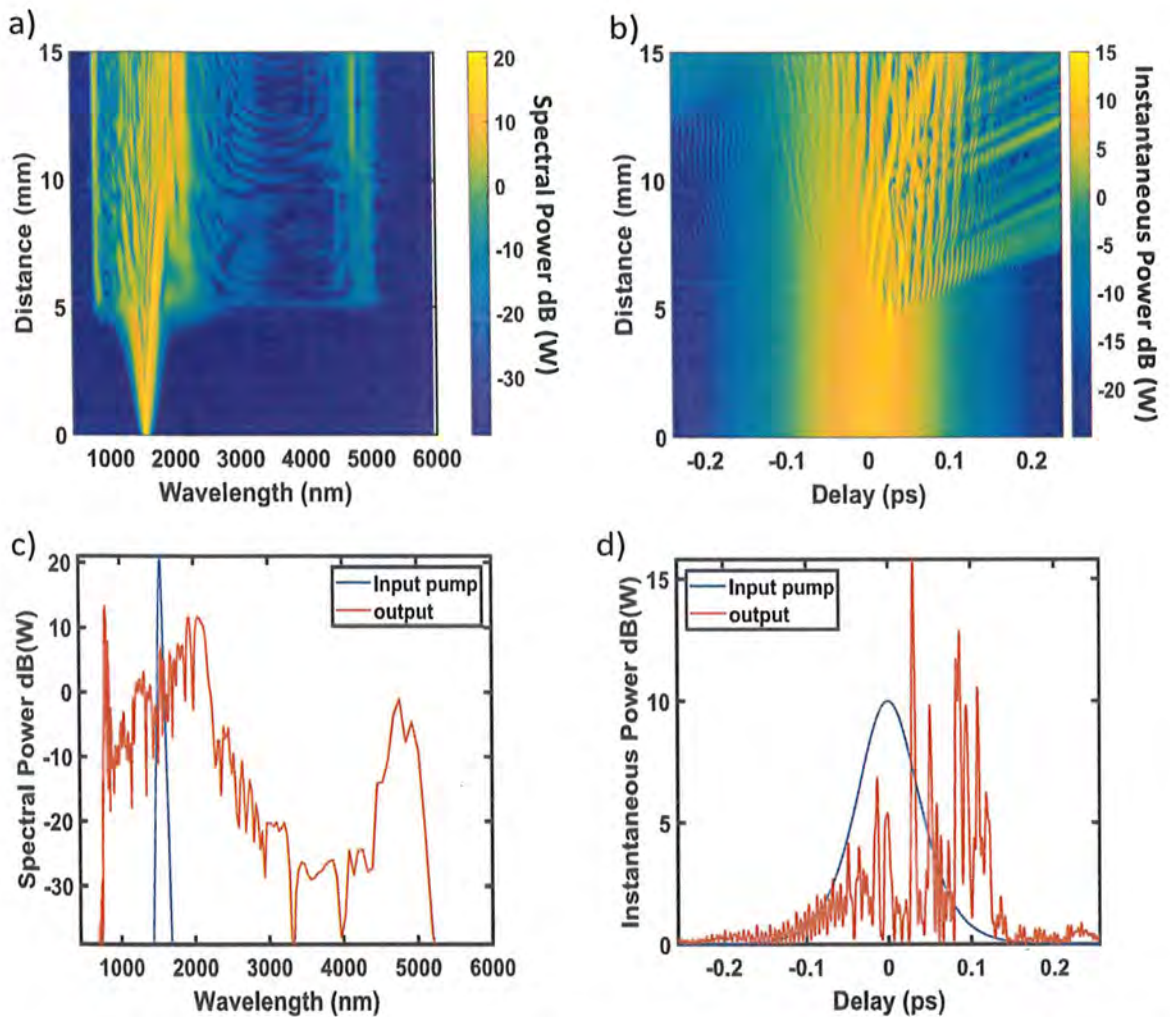Figure 3.1: The spectral and temporal representation of pulse evolution in dual-core waveguide structure with $0.5\mu m$ core height and $0.6\mu m$ gap spacing. **a)** The two-dimensional representation of the output pulse spectrum. **b)** The two-dimensional representation of the temporal delay. **c)** The spectral power of the input and output pulse. **d)** The instantaneous power of the input and output pulse.

to 4.7μm by engineering the dispersion profile of the dual-core Si$_2$N waveguide. It can be seen clearly that short-wavelength dispersive wave (SWDW) is obtained at 0.7μm wavelength while the long-wavelength dispersive wave (LWDW) is achieved at 4.7μm wavelength which represents the enhanced effects of supercontinuum at these wavelengths. The spectral power of output is then calculated as shown in figure (3.1 c) which illustrates that high power is achieved for the wavelengths where the long and short dispersive waves are generated.

The figure (3.1 b) illustrates that the input pulse experiences a temporal delay along the propagation due to the group velocity dispersion (GVD) and splits into high-intensity narrow-band pulses. It can be noted that the temporal compression of the pulse is initiated at around 5mm length of the waveguide. The instantaneous power of the propagating signal can be calculated at any distance z of the waveguide length. The figure (3.1 d) depicts the instantaneous pulse power measured at the waveguide's output end, which explains that the input pulse undergoes a linear phase shift due to GVD and splits into high-intensity narrowband pulses which can be described by the peak power of the splitted waves.

In figure (2.6) the calculations performed for dispersion phase profile of single core and dual-core waveguide structure with core height 0.8μm represents the extension of dispersive wave up to 6.4μm and 7.1μm in far-IR wavelength region respectively. The spectral and temporal evolution of the pulse as it propagates through the waveguide can be observed for these two geometries in figure (3.2) and figure (3.3) respectively.

The temporal delay experienced by the input pulse can be described in figure (3.2 b) for single core waveguide structure and in figure (3.3 b) for dual core waveguide structure which explains that the pump pulse starts spliting into four intense narrow band pulses at around 3.5mm waveguide length due to GVD. Whereas the spectral evolution of the pulse is shown in figure (3.2 a) and figure (3.3 a) which illustrates that spectral broadening also starts at around 3.5mm waveguide length.

The core height of 0.8μm thus proves very significant for shifting the barrier to extend

the dispersive wave generation up to $6.4\mu m$ with single-core waveguide and up to $7.1\mu m$ with dual-core waveguide structure. However, the flat dispersion curve is not achieved for these two geometries due to which the frequency components between $3\mu m$ to $6\mu m$ have no sufficient spectral power in supercontinuum which is presented in figure (3.2 c) and figure (3.3 c) respectively.
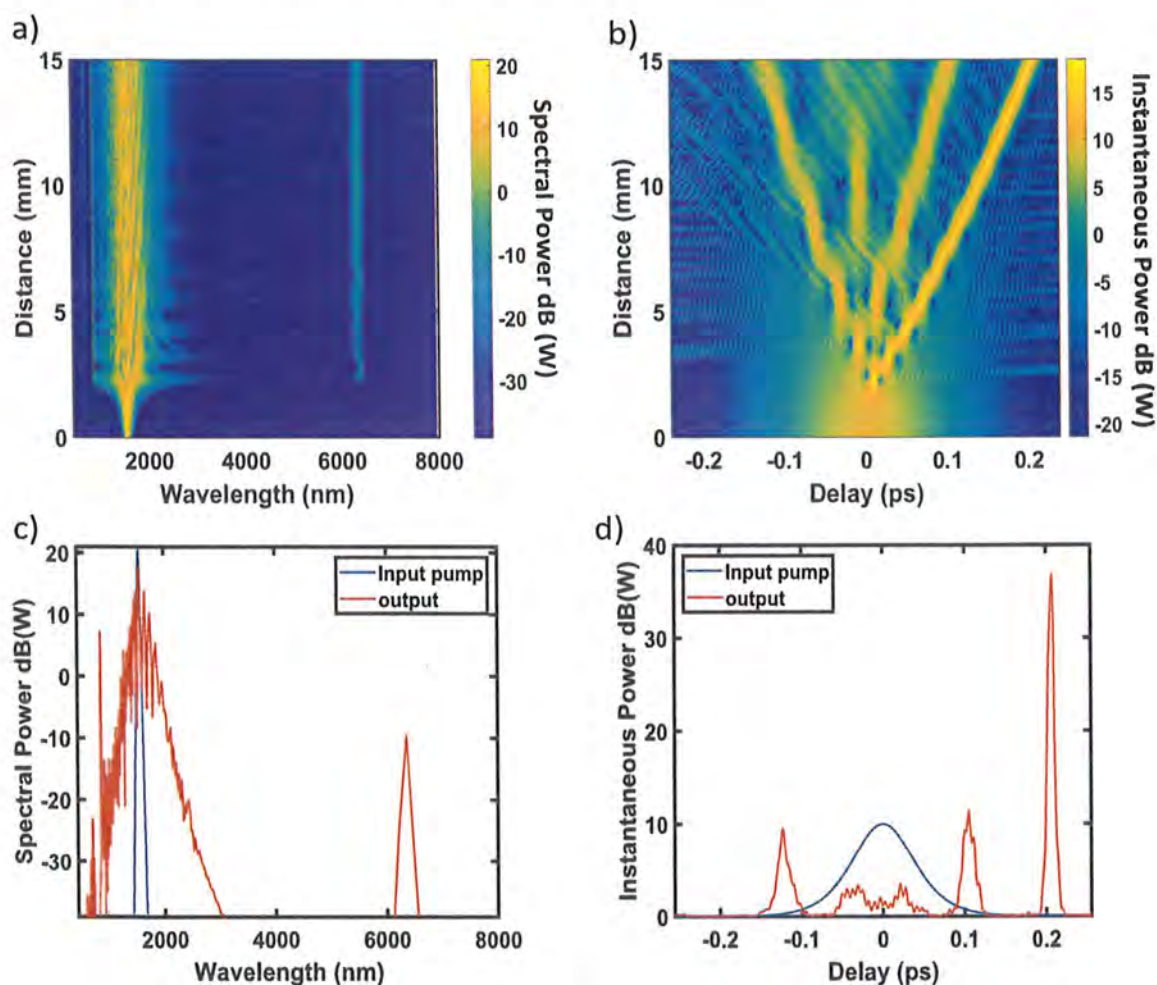
Figure 3.2: The spectral and temporal representation of pulse evolution in single-core waveguide structure with $0.8\mu m$ core height. **a)** The two-dimensional representation of the output pulse spectrum. **b)** The two-dimensional representation of the temporal delay. **c)** The spectral power of the input and output pulse. **d)** The instantaneous power of the input and output pulse.
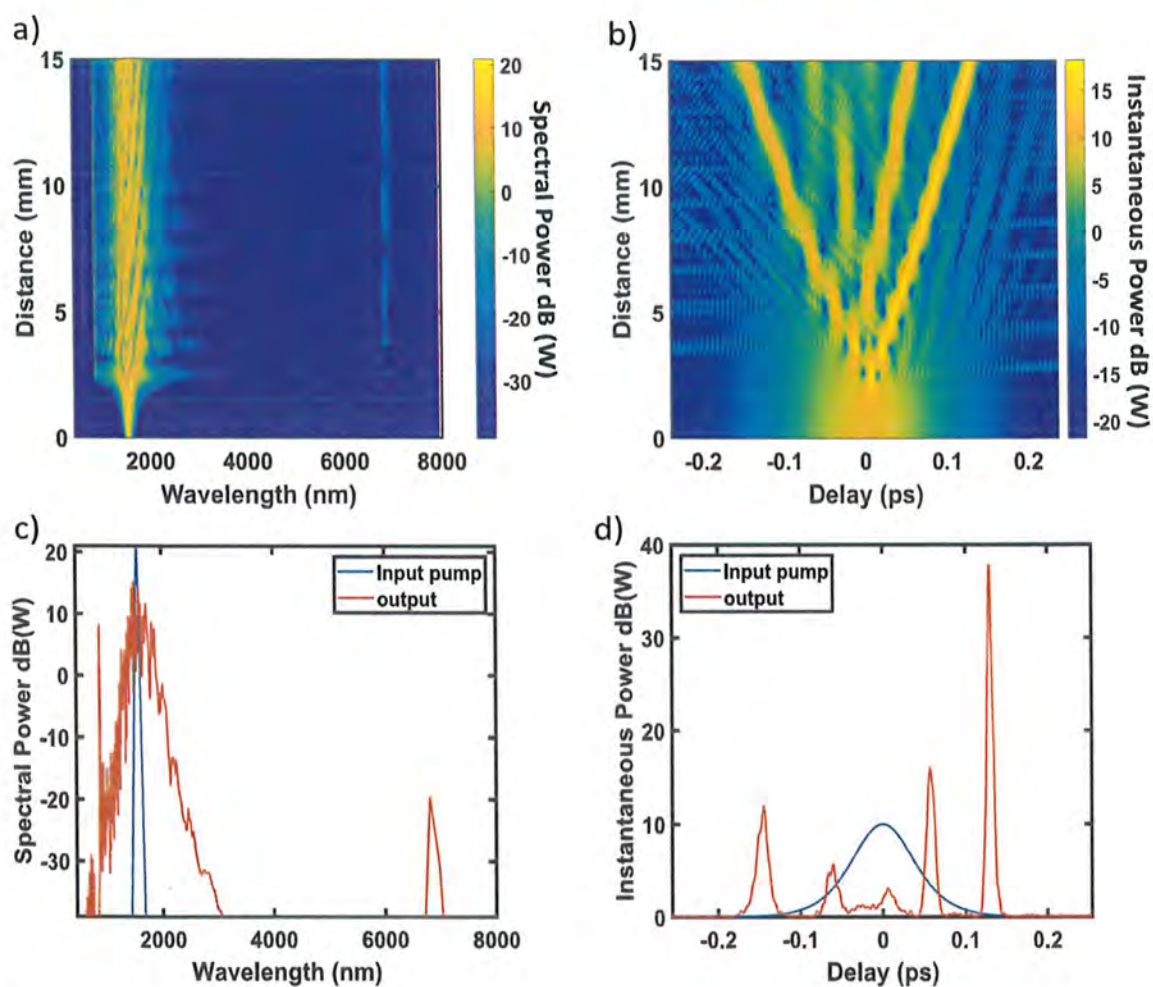
Figure 3.3: The spectral and temporal representation of pulse evolution in dual-core waveguide structure with $0.8\mu m$ core height and $1.7\mu m$ gap spacing. **a)** The two-dimensional representation of the output pulse spectrum. **b)** The two-dimensional representation of the temporal delay. **c)** The spectral power of the input and output pulse. **d)** The instantaneous power of the input and the output pulse.

In general, we observe the two main points in spanning of supercontinuum to mid-IR region; **the long wavelength edge** which can be extended by the dispersive wave generation in mid-IR or far-IR region by achieving phase matching of the propagation phase constant for the anti-symmetric mode of dual-core waveguide with respect to the propagation phase constant of pump pulse; **the moderate-wavelength part** between the dispersive wave at short wavelength (SWDW) and the dispersive wave at long wavelength (LWDW) which is done by the mode hybridization where the flat dispersion profile is targeted by reducing the overall phase mismatch. As a result, it can be observed that by increasing the gap distance between the two cores, the mid-IR dispersive wave is shifted to the longer wavelengths up to mid-IR or far-IR region.

In general, we observe the two main points in spanning of supercontinuum to mid-IR region; **the long wavelength edge** which can be extended by the dispersive wave generation in mid-IR or far-IR region by achieving phase matching of the propagation phase constant for the anti-symmetric mode of dual-core waveguide with respect to the propagation phase constant of pump pulse; **the moderate-wavelength part** between the dispersive wave at short wavelength (SWDW) and the dispersive wave at long wavelength (LWDW) which is done by the mode hybridization where the flat dispersion profile is targeted by reducing the overall phase mismatch. As a result, it can be observed that by increasing the gap distance between the two cores, the mid-IR dispersive wave is shifted to the longer wavelengths up to mid-IR or far-IR region.

Chapter 4

Conclusion and Future Work

4.1 Conclusion

In this thesis we have investigated the simulation based results for spanning of the broadband supercontinuum generation up to the mid-IR region by engineering the dispersion profile of the silicon-rich nitride dual-core waveguide. The behaviour of waveguide dispersion (D_{wg}) and integrated dispersion ($\Delta\beta$) have been analysed for both $0.5\mu m$ and $0.8\mu m$ core height of the dual-core waveguide. It is noted that supercontinuum spanning is extended beyond $4\mu m$ and in the meantime, the flat dispersion profile is also achieved from $1.2\mu m$ to $2.2\mu m$ in the near-IR region for the dual-core waveguide with core height of $0.5\mu m$. Moreover, by varying the gap spacing between two cores the dispersive wave location also changes. Results describe that the dispersive wave is achieved at $4.7\mu m$ wavelength for $0.5\mu m$ core height whereas for $0.8\mu m$ core height the dispersive wave generation is extended up to $7.1\mu m$ wavelength in far-IR region, however the flat dispersion profile is not achieved in that case. This is the widest SCG spanning using planar silicon-rich nitride waveguide structure to the best of our knowledge which can be used in various mid-IR applications.

4.2   Future Insight

For the future work we are interested to study the dispersion-engineering in multi-core waveguide structure to enhance the optical power of spectral components achieved in the broad-band supercontinuum source generation at the waveguide output. The significant coupling is seen for dual-core and tri-core waveguide structures which are represented by the figures below and it is expected that the multi-core waveguide structure would give interesting results to investigate.

(a)   (b)
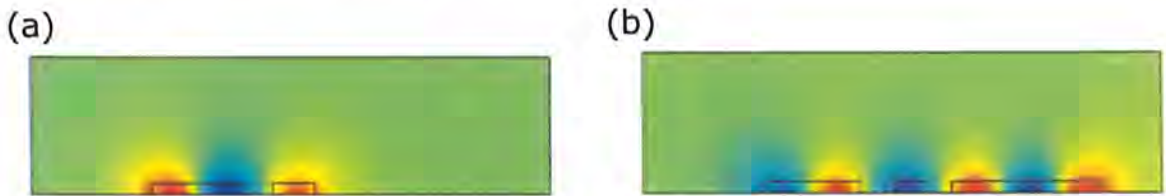
Figure 4.1: a)The mode coupling in dual-core waveguide structures. b)The mode coupling in tri-core waveguide structures.

In addition to dispersion-engineering we are also interested to study the interaction of two-dimensional materials with dual-core planar waveguide structure to maximize the spectral coverage of Supercontinuum. By interfacing the 2D material layer with the photonic integrated waveguide it is expected that we can tune the refractive indices of the waveguide spacing by applying voltage because the two-dimensional materials have diverse optical properties and the ability to control charge carriers when potential is applied. In this way we can fabricate only one dual-core waveguide structure with the deposition of 2D material layer instead of fabricating different waveguide structures with different gap spacing on a single photonic chip. This is very promising in terms of efficiency and cost-effectiveness.

References

[1] J. M. Dudley and J. R. Taylor, *Supercontinuum generation in optical fibers.* Cambridge University Press, 2010.

[2] O. Boyraz, T. Indukuri, and B. Jalali, "Self-phase-modulation induced spectral broadening in silicon waveguides," *Optics Express*, vol. 12, no. 5, pp. 829–834, 2004.

[3] E. Dulkeith, Y. A. Vlasov, X. Chen, N. C. Panoiu, and R. M. Osgood, "Self-phase-modulation in submicron silicon-on-insulator photonic wires," *Optics express*, vol. 14, no. 12, pp. 5524–5534, 2006.

[4] B. Stuart, "Infrared spectroscopy," *Kirk-Othmer encyclopedia of chemical technology*, 2000.

[5] I. Vurgaftman, C. L. Canedy, C. S. Kim, M. Kim, W. W. Bewley, J. R. Lindle, J. Abell, and J. R. Meyer, "Mid-infrared interband cascade lasers operating at ambient temperatures," *New Journal of Physics*, vol. 11, no. 12, p. 125015, 2009.

[6] Y. Yao, A. J. Hoffman, and C. F. Gmachl, "Mid-infrared quantum cascade lasers," *Nature Photonics*, vol. 6, no. 7, pp. 432–439, 2012.

[7] F. Jerome, F. Capasso, D. L. Sivco, C. Sirtori, A. L. Hutchinson, and A. Y. Cho, "Quantum cascade laser," *Science*, vol. 264, no. 5158, pp. 553–556, 1994.

[8] G. Villares, A. Hugi, S. Blaser, and J. Faist, "Dual-comb spectroscopy based on quantum-cascade-laser frequency combs," *Nature communications*, vol. 5, no. 1, pp. 1–9, 2014.

[9] F. Keilmann and S. Amarie, "Mid-infrared frequency comb spanning an octave based on an er fiber laser and difference-frequency generation," *Journal of Infrared, Millimeter, and Terahertz Waves*, vol. 33, no. 5, pp. 479–484, 2012.

[10] F. C. Cruz, D. L. Maser, T. Johnson, G. Ycas, A. Klose, F. R. Giorgetta, I. Coddington, and S. A. Diddams, "Mid-infrared optical frequency combs based on difference frequency generation for molecular spectroscopy," *Optics express*, vol. 23, no. 20, pp. 26 814–26 824, 2015.

[11] S. A. Diddams, T. Udem, J. Bergquist, E. Curtis, R. Drullinger, L. Hollberg, W. M. Itano, W. Lee, C. Oates, K. Vogel *et al.*, "An optical clock based on a single trapped 199hg+ ion," *Science*, vol. 293, no. 5531, pp. 825–828, 2001.

[12] A. Schliesser, M. Brehm, F. Keilmann, and D. W. van der Weide, "Frequency-comb infrared spectrometer for rapid, remote chemical sensing," *Optics Express*, vol. 13, no. 22, pp. 9029–9038, 2005.

[13] X. Pang, O. Ozolins, R. Schatz, J. Storck, A. Udalcovs, J. R. Navarro, A. Kakkar, G. Maisons, M. Carras, G. Jacobsen *et al.*, "Gigabit free-space multi-level signal transmission with a mid-infrared quantum cascade laser operating at room temperature," *Optics letters*, vol. 42, no. 18, pp. 3646–3649, 2017.

[14] I. Hartl, X. Li, C. Chudoba, R. Ghanta, T. Ko, J. Fujimoto, J. Ranka, and R. Windeler, "Ultrahigh-resolution optical coherence tomography using continuum generation in an air–silica microstructure optical fiber," *Optics letters*, vol. 26, no. 9, pp. 608–610, 2001.

[15] D. J. Jones, S. A. Diddams, J. K. Ranka, A. Stentz, R. S. Windeler, J. L. Hall, and S. T. Cundiff, "Carrier-envelope phase control of femtosecond mode-locked lasers and direct optical frequency synthesis," *Science*, vol. 288, no. 5466, pp. 635–639, 2000.

[16] P. Corrigan, R. Martini, E. A. Whittaker, and C. Bethea, "Quantum cascade lasers and the kruse model in free space optical communication," *Optics Express*, vol. 17, no. 6, pp. 4355–4359, 2009.

[17] A. Schliesser, N. Picqué, and T. W. Hänsch, "Mid-infrared frequency combs," *Nature photonics*, vol. 6, no. 7, pp. 440–449, 2012.

[18] A. G. Griffith, R. K. Lau, J. Cardenas, Y. Okawachi, A. Mohanty, R. Fain, Y. H. D. Lee, M. Yu, C. T. Phare, and C. B. Poitras, "Silicon-chip mid-infrared frequency comb generation," *Nature communications*, vol. 6, no. 1, pp. 1–5, 2015.

[19] M. Yu, Y. Okawachi, A. G. Griffith, N. Picqué, M. Lipson, and A. L. Gaeta, "Silicon-chip-based mid-infrared dual-comb spectroscopy," *Nature communications*, vol. 9, no. 1, pp. 1–6, 2018.

[20] C. Y. Wang, T. Herr, P. Del'Haye, A. Schliesser, J. Hofer, R. Holzwarth, T. Hänsch, N. Picqué, and T. J. Kippenberg, "Mid-infrared optical frequency combs at 2.5 μm based on crystalline microresonators," *Nature communications*, vol. 4, no. 1, pp. 1–7, 2013.

[21] K. Luke, Y. Okawachi, M. R. Lamont, A. L. Gaeta, and M. Lipson, "Broadband mid-infrared frequency comb generation in a si 3 n 4 microresonator," *Optics letters*, vol. 40, no. 21, pp. 4823–4826, 2015.

[22] S. T. Cundiff and J. Ye, "Colloquium: Femtosecond optical frequency combs," *Reviews of Modern Physics*, vol. 75, no. 1, p. 325, 2003.

[23] B. Kuyken, T. Ideguchi, S. Holzner, M. Yan, T. W. Hänsch, J. Van Campenhout, P. Verheyen, S. Coen, F. Leo, R. Baets *et al.*, "An octave-spanning mid-infrared frequency comb generated in a silicon nanophotonic wire waveguide," *Nature communications*, vol. 6, no. 1, pp. 1–6, 2015.

[24] N. Singh, D. D. Hudson, Y. Yu, C. Grillet, S. D. Jackson, A. Casas-Bedoya,

A. Read, P. Atanackovic, S. G. Duvall, S. Palomba *et al.*, "Midinfrared supercontinuum generation from 2 to 6 μm in a silicon nanowire," *Optica*, vol. 2, no. 9, pp. 797–802, 2015.

[25] D. Y. Oh, D. Sell, H. Lee, K. Y. Yang, S. A. Diddams, and K. J. Vahala, "Supercontinuum generation in an on-chip silica waveguide," *Optics letters*, vol. 39, no. 4, pp. 1046–1048, 2014.

[26] D. Y. Oh, K. Y. Yang, C. Fredrick, G. Ycas, S. A. Diddams, and K. J. Vahala, "Coherent ultra-violet to near-infrared generation in silica ridge waveguides," *Nature communications*, vol. 8, no. 1, pp. 1–7, 2017.

[27] J. Lu, J. B. Surya, X. Liu, Y. Xu, and H. X. Tang, "Octave-spanning supercontinuum generation in nanoscale lithium niobate waveguides," *Optics letters*, vol. 44, no. 6, pp. 1492–1495, 2019.

[28] M. Yu, B. Desiatov, Y. Okawachi, A. L. Gaeta, and M. Lončar, "Coherent two-octave-spanning supercontinuum generation in lithium-niobate waveguides," *Optics letters*, vol. 44, no. 5, pp. 1222–1225, 2019.

[29] S. May, M. Clerici, and M. Sorel, "Supercontinuum generation in dispersion engineered algaas-on-insulator waveguides," *Scientific Reports*, vol. 11, no. 1, pp. 1–7, 2021.

[30] B. Kuyken, M. Billet, F. Leo, K. Yvind, and M. Pu, "Octave-spanning coherent supercontinuum generation in an algaas-on-insulator waveguide," *Optics letters*, vol. 45, no. 3, pp. 603–606, 2020.

[31] D. D. Hickstein, H. Jung, D. R. Carlson, A. Lind, I. Coddington, K. Srinivasan, G. G. Ycas, D. C. Cole, A. Kowligy, C. Fredrick *et al.*, "Ultrabroadband supercontinuum generation and frequency-comb stabilization using on-chip waveguides with both cubic and quadratic nonlinearities," *Physical Review Applied*, vol. 8, no. 1, p. 014025, 2017.

[32] J. Lu, X. Liu, A. W. Bruch, L. Zhang, J. Wang, J. Yan, and H. X. Tang, "Ultraviolet to mid-infrared supercontinuum generation in single-crystalline aluminum nitride waveguides," *Optics Letters*, vol. 45, no. 16, pp. 4499–4502, 2020.

[33] A. R. Johnson, A. S. Mayer, A. Klenner, K. Luke, E. S. Lamb, M. R. Lamont, C. Joshi, Y. Okawachi, F. W. Wise, M. Lipson *et al.*, "Octave-spanning coherent supercontinuum generation in a silicon nitride waveguide," *Optics letters*, vol. 40, no. 21, pp. 5117–5120, 2015.

[34] D. R. Carlson, D. D. Hickstein, A. Lind, S. Droste, D. Westly, N. Nader, I. Coddington, N. R. Newbury, K. Srinivasan, S. A. Diddams *et al.*, "Self-referenced frequency combs using high-efficiency silicon-nitride waveguides," *Optics letters*, vol. 42, no. 12, pp. 2314–2317, 2017.

[35] H. Guo, C. Herkommer, A. Billat, D. Grassani, C. Zhang, M. H. Pfeiffer, W. Weng, C.-S. Bres, and T. J. Kippenberg, "Mid-infrared frequency comb via coherent dispersive wave generation in silicon nitride nanophotonic waveguides," *Nature Photonics*, vol. 12, no. 6, pp. 330–335, 2018.

[36] H. Guo, W. Weng, J. Liu, F. Yang, W. Hänsel, C. S. Brès, L. Thévenaz, R. Holzwarth, and T. J. Kippenberg, "Nanophotonic supercontinuum-based mid-infrared dual-comb spectroscopy," *Optica*, vol. 7, no. 9, pp. 1181–1188, 2020.

[37] D. Tan, K. Ooi, and D. Ng, "Nonlinear optics on silicon-rich nitride—a high nonlinear figure of merit cmos platform," *Photonics Research*, vol. 6, no. 5, pp. B50–B66, 2018.

[38] M. Karim, N. Al Kayed, and B. Rahman, "Broadband supercontinuum generation in the mid-infrared range (0.8 μm–4.5 μm) using low power dispersion-engineered linbo3 cladded silicon-rich nitride waveguide," in *2020 IEEE Region 10 Symposium (TENSYMP)*. IEEE, 2020, pp. 246–249.

[39] M. Yang, L. Xu, J. Wang, H. Liu, X. Zhou, G. Li, and L. Zhang, "An octave-spanning optical parametric amplifier based on a low-dispersion silicon-rich nitride waveguide," *IEEE Journal of Selected Topics in Quantum Electronics*, vol. 24, no. 6, pp. 1–7, 2018.

[40] D. E. Zelmon, D. L. Small, and D. Jundt, "Infrared corrected sellmeier coefficients for congruently grown lithium niobate and 5 mol.% magnesium oxide–doped lithium niobate," *JOSA B*, vol. 14, no. 12, pp. 3319–3322, 1997.

[41] M. Pu, L. Liu, H. Ou, K. Yvind, and J. M. Hvam, "Ultra-low-loss inverted taper coupler for silicon-on-insulator ridge waveguide," *Optics Communications*, vol. 283, no. 19, pp. 3678–3682, 2010.

[42] X. Liu and B. Lee, "A fast method for nonlinear schrodinger equation," *IEEE Photonics Technology Letters*, vol. 15, no. 11, pp. 1549–1551, 2003.

[43] C. Bayindir, "Compressive split-step fourier method," *TWMS Journal of Applied and Engineering Mathematics*, vol. 5, no. 2, pp. 298–306, 2015.

Turnitin Originality Report

DISPERSION ENGINEERED MID-IR SUPERCONTINUUM GENERATION USING DUAL-CORE SILICON-RICH NITRIDE PHOTONIC INTEGRATED WAVEGUIDE by Kiran Ilyas .

From DRSM (DRSM L)

- Processed on 20-Apr-2021 23:37 PKT
- ID: 1564901341
- Word Count: 4270

Similarity Index
2%
Similarity by Source

Internet Sources:
 1%
Publications:
 2%
Student Papers:
 0%

sources:

1 1% match (publications)

Rui Ma, Kuiru Wang, Shipei Jing, Chao Mei, Jinhui Yuan, Chongxiu Yu, Binbin Yan, Xinzhu Sang. "Experimental Demonstration of 3-bit All-optical Quantization Based on Slicing Supercontinuum Spectrum", 2018 Asia Communications and Photonics Conference (ACP), 2018

2 < 1% match (Internet from 11-Apr-2020)

https://worldwidescience.org/topicpages/c/curved+waveguide+arrays.html

3 < 1% match (publications)

Libin Fu, Brian K. Thomas, Liang Dong. "Efficient supercontinuum generations in silica suspended core fibers", Optics Express, 2008

4 < 1% match (publications)

Juanjuan Lu, Joshua B. Surya, Xianwen Liu, Yuntao Xu, Hong X. Tang. "Octave-spanning supercontinuum generation in nanoscale lithium niobate waveguides", Optics Letters, 2019

5 < 1% match (Internet from 14-Mar-2020)

https://eprints.soton.ac.uk/348818/1/Rami%2520Saba%2520Thesis%25202012.pdf

paper text:

DISPERSION ENGINEERED MID-IR SUPERCONTINUUM GENERATION USING DUAL-CORE SILICO RICH NITRIDE PHOTONIC INTEGRATED WAVEGUIDE QUAID-I-AZAM UNIVERSITY ISLAMABAD By Kiran Ilyas Abstract The dual core silicon-rich nitride photonic integrated waveguide is presented here to numerically model the spanning of supercontinuum generation in mid-IR region particularly up to 4.7μm wavelength range by engineering the dispersion profile such that maximum phase matching can be achieved in mid-IR region. The flat dispersion profile is also achieved to some extent in the near-IR regior